Supporting Information

"Total shortening estimates across the Western Greater Caucasus Mountains from balanced cross sections and area balancing" by Trexler et al. – TEKTONIKA 2023

Figure SI-1. Geologic map of the Enguri Traverse, western Greater Caucasus (long dimension 108 cm). Bold band in center delineates the 1:100k mapping transect of Trexler et al. (2022), with a base map compiled from 1:200k geologic maps (Trexler et al., 2022). Stereograms show poles to bedding planes in an equal area projection and use a Kamb contour with an interval of 5.

Figure SI-2. Tectonostratigraphic column for units on the Enguri Traverse, reproduced from Trexler et al. (2022). Unit descriptions are compiled from outcrops, hand samples, and thin sections. Unit thicknesses are estimated based on mapping and structural data. References for mapped age: 1. Gamkrelidze and Kakhazdze (1959). 2. Vasey et al. (2020). 3. Dzhanelidze and Kandelaki (1957). 4. Kandelaki (1957).

Figure SI-3. Geologic map of the Terek-Aragvi Traverse, central Greater Caucasus (long dimension 108 cm). Bold band in center delineates the 1:100k mapping transect of Trexler et al. (2022), with a base map compiled from 1:200k geologic maps (Trexler et al., 2022). Stereograms show poles to bedding planes (or, in the case of the Gveleti domain, foliation in gneiss) in an equal area projection, and use a Kamb contour with an interval of 5.

Figure SI-4. Tectonostratigraphic column for units on the Terek-Aragvi Traverse, reproduced from Trexler et al. (2022). Unit descriptions are compiled from outcrops, hand samples, and thin sections. Unit thicknesses are estimated based on mapping and structural data. References for mapped age: 1. Vasey et al., 2020 2. Gubkina and Ermakov, 1989. 3. Kandelaki and Kakhazdze, 1957.

Methods for balanced cross section construction and restoration

We constructed our balanced cross sections to represent surface geology and structural data at 1:200,000 scale, using simplified tectonostratigraphic units based upon those of Trexler et al. (2022). Structural data and stratigraphic observations used to guide construction of cross sections are previously published in Trexler et al. (2022), and reproduced here in figures SI-1-SI-4.

In cross section construction, we intentionally make decisions to minimize shortening, such that the final shortening values from our cross sections across the orogen are robust minimum estimates. In accordance with this strategy, we make several fundamental assumptions: (1) units are laterally continuous, (2) units maintain constant thickness, (3) units are juxtaposed by faults that cut bedding-parallel or up-section, but not down-section, and (4) where unpreserved, hanging wall cutoffs are immediately adjacent but have been eroded. We acknowledge that these assumptions are simplistic and, in the case of (1) and (2) unlikely to apply over the ≥200 km length scales of these cross sections. However, currently available data are insufficient to determine stratigraphic thicknesses at multiple locations along each section. We define unit thicknesses in cross section using the maximum thickness for each unit as determined from our field observations and map patterns reported by Trexler et al. (2022) [Figures SI-1 and SI-2]. To avoid competing assumptions that may unintentionally distort our shortening estimates, we intentionally bias each assumption toward minimizing the resulting shortening estimate.

We model fold geometries using the fault bend fold model of Suppe (1983). Guided by field observations and structural measurements (Trexler et al., 2022) we default to ramp and backlimb dips of 30° and forelimb dips of 50°, consistent with Suppe (1983). We use this default fault bend fold geometry as a template, with which we construct all geometric relationships in each section in a manner that matches, as near as possible, surface observations of geologic units and bedding orientations reported in Trexler et al. (2022) and Mosar et al. (2022) [Figures SI-1 and SI-2]. Wherever possible, we correlate stratigraphic units using direct field observation of rock type (Trexler et al., 2022) in conjunction with published biostratigraphic age data (Gamkrelidze & Kakhazdze, 1959; Gubkina & Ermakov, 1989). For areas without primary structural data, we defer to unit correlations and ages from published geologic maps (Gamkrelidze & Kakhazdze, 1959; Gubkina & Ermakov, 1989). Along both traverses, strata younger than ~30 Ma are syntectonic deposits (Banks et al., 1997; Dzhanelidze & Kandelaki, 1957; Kandelaki & Kakhazdze, 1957), and we do not extend them continuously across the orogen as part of the pre-tectonic sequence. This is consistent with 1:200,000 scale geologic mapping indicating that units within the range are nearly all Mesozoic or older in age (Gamkrelidze & Kakhazdze, 1959; Gubkina & Ermakov, 1989). In keeping with this observation, we assume that syntectonic strata, where not exposed in the core of the range, should not be incorporated into thrust sheets.

Notes on Enguri section (Figure 2).

1. The Idliani, Khaishi, Dizi, Mestia, and Ushba faults have no unit correlation across them, and thus could accommodate significantly more shortening than we attribute to them. The restored section is constructed as if unpreserved hangingwall cutoffs are immediately adjacent to the eroded topography, to minimize estimated shortening in the restored section.
2. Though a fault is mapped north of the Ushba fault, and we represent it in our unrestored section, the geometry of and displacement across the structure are unclear. Thus, as we are attempting to define an absolute minimum shortening estimate, we do not include any shortening across this structure in our restoration.

3. The contact between the sedimentary section and crystalline basement is likely irregular, and juxtaposes different parts of the section against basement, as supported by the exposure of basement to the west of the line of profile at the north end of the swath. However, without any constraint on the nature of this contact, we have represented it as planar in our cross sections. We note that the nature of this contact has no direct influence on the amount of shortening accommodated in the cross section.
4. Neogene and younger sediments are considered syn-orogenic and not incorporated into the restored section except where explicitly deformed in foreland fold/thrust belt(s).

Notes on Aragvi section (Figure 3).

1. The Ananuri, Pasanauri, Gudauri, Gveleti, and Terek faults have no unit correlation across them, and thus could accommodate significantly more shortening than we attribute to them. The restored section is constructed as if unpreserved hangingwall cutoffs are immediately adjacent to the eroded topography, to minimize estimated shortening in the restored section.
2. Neogene and younger sediments are considered syn-orogenic and not incorporated into the restored section except where explicitly deformed in foreland fold/thrust belt(s).

Notes on Area Balancing Methods

For the cross-sectional areas across the modern GC, we extract mean elevation from 30-m-resolution ASTER digital elevation data (https://doi.org/10.5067/ASTER/AST14DEM.003) along a 10 km-wide, orogen-perpendicular swath running the length of the section. Approximated Moho depths are interpolated from teleseismic tomography estimates (Zor, 2008) and incorporate the approximate geometry and location of the subducted slab reported by Mumladze et al. (2015). We define end-member values for the thickness of the crust prior to the onset of shortening using modern crustal thickness of the Eastern Black Sea and the Scythian Platform for the cases of initial oceanic and continental crust, respectively (Yegorova et al., 2010).

Any use of trade, firm, or product names is for descriptive purposes only and does not imply endorsement by the U.S. Government.


a
Kilometers
0
5
10
20
30
40
detailed map border (banel b)
b
Rioni Basin Fold Thrust Belt
Idliani Fault
Khaishi Fault
Dizi Fault
Ushba Fault
Zugdidi
N
Compiled from 1:200,000 regional geology:
Cenozoic
Q Quaternary
N2
N1 Neogene
Pg3
Pg2 Paleogene
Pg1
Mesozoic
K2
K1 Cretaceous
J2
J1 Jurassic
Ji Jurassic (intrusive)
Tr Triassic
Paleozoic
C Carboniferous
D Devonian
S Silurian
Pz Paleozoic (undifferentiated)
Pzb Paleozoic crystalline basement
Enguri Traverse Tectonostratigraphy (Trexler et al., 2022):
E-jl
E-js
E-jv
E-iv
E-kv
E-ks
E-ds2
E-ds1
E-xb
0
5
10 km
Jvari Domain
Idliani Domain
Khaishi Domain
Dizi Domain
Ushba Domain
Age
0-10 Ma
10-50 Ma
50-100 Ma
>100 Ma
Apatite (U-Th)/He
Apatite Fission Track
modified from Banks et al., 1997
Tsaishi Anticline
Elevation above sea level (km)
Figure SI-

Lithostratigraphy - Enguri River Traverse *(Trexler et al., 2022)*

Domain	Unit	Outcrop & Hand Sample:	Petrography:	Previously Mapped Age:
Jvari Domain	E-jls	thick fossiliferous limestone, forms flatiron-like rangefront. Local complex deformation	sedimentary: - volcanic lithic grains - carbonate cement volcanic: - altered but texturally pristine volcanic - euhedral feldspars - hornblende - biotite - orthopyroxene - amygdules with calcite and zeolite facies minerals	K1
	E-js	mudstone, shales and sandstone with occasional massive debris flows getting thicker and more regular moving down section. Mudstones often contain organic matter including petrified wood		J2
	E-jv	massive, coarse, angular volcanic breccias compositionally similar to debris flows found in E-js. Occasional moderate-composition intrusive dikes, particularly lower in section. Sandtone-shale horizons (generally 1-10m thick) present in upper part of section. Flow direction broadly north.		
Idliani Fault				
Idliani Domain	E-iv	poorly exposed, creating less relief than other units along section. In outcrop, similar to E-jv, E-kv and E-ks. Angular, arkosic fine sandstones. Finer grained than E-ks; sed structures present but less obvious than in E-ks.	sedimentary: - volcanic lithic grains - quartz grains exhibit undulose extinction - fragments of multigranular quartz volcanic: - primary textures preserved - contain two pyroxenes	J2
Khaishi Fault				
Khaishi Domain	E-kv	volcanic breccias, mudstone and sandstone. occasional very resistant beds form dramatic ribs in landscape, which provide bedding orientation. Several horizons contain pillow basalts. Some volcaniclastics contain mm-scale px phenocrysts and several-cm volcanic lithic clasts.	altered but texturally pristine two pyroxenes	J2
	E-ks	fine grain sandstone and slate, often exhibiting well developed graded bedding and other sedimentary structures. Mostly fine sands and muds with intermittent ~1m thick arkosic sand beds (some contain qtz and muscovite) becoming more frequent moving up section. Flow direction broadly south	quartz grains exhibit undulose extinction metasedimentary lithic grains detrital muscovite	J1
Dizi Fault				
Dizi Domain	E-ds2	medium to fine meta-sandstone and phyllite. Graded beds and other sedimentary structures. Well developed cleavage. Crenulations present in some outcrops.	quartz grains exhibit undulose extinction detrital muscovite	Pz
	E-ds1	metasandstones, slates and phyllites. Subvertical bedding; facing direction often difficult to determine. Very well developed cleavage. Thought to correspond to Dizi Series [*Adamia et al.*, 2011]		
Ushba Fault				
Ushba Domain	E-ux	gneisses, grantic intrusives (which also in places exhibit compositional banding), and metasedimentary schist. Locally, migmatitic deformation, especially in immediate hanging wall of Ushba Thrust.		Pz

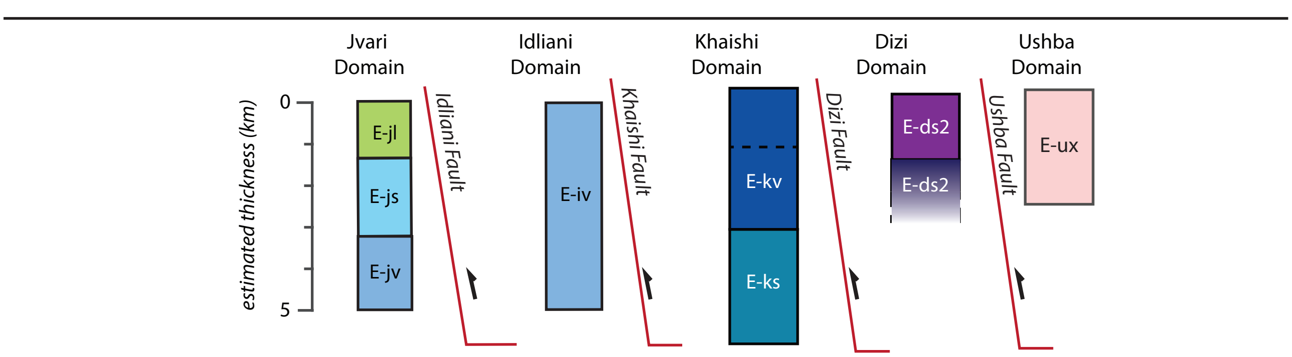

Figure SI-2


a
42°0'0"N
42°30'0"N
44°30'0"E
43°0'0"N
43°30'0"N
45°0'0"E
detailed map border (banel b)
detailed map border (banel b)
Kilometers
0 5 10 20 30 40
b
Compiled from 1:200,000 regional geology:
Cenozoic
Q Quaternary
Qv Quaternary volcanic
N2
N1
Neogene
Pg3
Pg2
Paleogene
Czi Cenozoic igneous
Mesozoic
K2
K1
Cretaceous
J3
J2
J1
Jurassic
Paleozoic
Pz Paleozoic (undifferentiated)
Jinvali Domain
Ananuri Domain
Pasanauri Domain
Gveleti Domain
0 5 10 km
Ananuri Fault
Pasanauri Fault
Gveleti Fault
strip map border (panel a)
strip map border (panel a)
Jinvali
Pasanauri
Gudauri
Truso Valley
Kazbeg
Stepantsminda
Sno
CT15113
CT15092
AB0938
Aragvi/Terek Traverse Tectonostratigraphy (Trexler et al., 2022):
Age
0-10 Ma
10-50 Ma
50-100 Ma
>100 Ma
Apatite (U/Th)-He
Apatite Fission Track
CT15113
5.13 +/- 0.81
CT15092
6.97 +/- 0.06
AB0938
2.7 +/- 0.4
modified from Banks et al. 1997
Kvernaki Anticline
Jvari Pass
form line
elevation above sea level (km)

Figure SI-3

Lithostratigraphy - Aragvi River Traverse (Trexler et al., 2022)

Domain	Unit	Outcrop & Hand Sample:	Petrography:	Previously Mapped Age:
Jinvali Domain	A-js2	shale, sandstone and pebble conglomerate. Contain large olistoliths of massive carbonate (likely A-jls)	- dominated by fossil fragments - subangular qartz grains with undulatory extinction - microcrystalline quartz grains	N1
Jinvali Domain	A-jls	massive, blue-grey limestone		K
Jinvali Domain	A-js1	poorly lithified and poorly exposed black shale and mudstone		J1
Ananuri Thrust				
Ananuri Domain	A-as2	thinly bedded (~10cm - .5m) limestone with dark shale interbeds; often complexly deformed esp. near large structures		K2
Ananuri Domain	A-as1	interbedded sandstone and dark shale, often .5 - 2m thick. Grading and crossbeds present but often difficult to distinguish. Trace fossils at base of sandy beds in upper part of section. Poorly developed cleavage.	- detrital mica present but rare - grains very well rounded - plagioclase - lithic fragments - multigranular quartz grains - contians rare microcline grains - some samples contain abundant fossil fragments	K1
Pasanauri Thrust				
Pasanauri Domain	A-ps3	sandstone and slate, occasionally with carbonate cement. Well developed scours and load casts on sand bed bases. Moderately developed cleavage	- quartz grains do not exhibit undulose extinction - feldspars altered - detrital muscovites appear bent around other grains - grains more rounded in sections near Pasanauri Fault (further south)	J3
Pasanauri Domain	A-ps2	dark grey slate. Well-developed cleavage almost always present	- plagioclase (less altered than in A-ps1) - quartz grains exhibit undulose extinction - microcline - detrital muscovite - finer grained samples show incipient fabric and pyrite framboids - calcite cement	J2
Pasanauri Domain	A-ps1	slate to phyllite. Well developed cleavage often more prominent than bedding. Prevalent secondary mineral growth, including quartz veins and equant pyrite (up to ~cm scale)	- quartz grains do not exhibit undulose extinction - plagioclase (altered) - fragments of multigranular quartz (chert?) - detrital muscovite present but uncommon	J1
Gveleti Thrust				
Gveleti Domain	A-gs	Phyllite. Well developed cleavage. Prevalent secondary mineral growth, including quartz veins and equant pyrite (up to ~cm scale)	- quartz grains exhibit undulose extinction - plagioclase (altered)	J1
Gveleti Domain	A-gx	gneiss with subvertical intrusive dikes, subvertical compositional banding		Pz

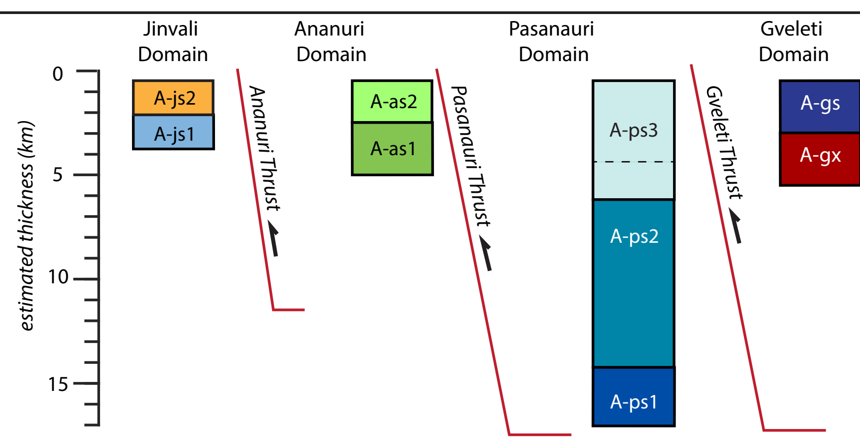

Figure SI-4